

1 **Title:** Microfluidic-controlled manufacture of liposomes for the solubilisation of a
2 poorly water soluble drug.

3

4 **Authors:** Elisabeth Kastner, Varun Verma, Deborah Lowry and Yvonne Perrie*

5

6

7 Aston Pharmacy School, School of Life and Health Sciences, Aston University,
8 Birmingham, UK, B4 7ET.

9

10

11

12

13 *Correspondence: Professor Yvonne Perrie
14 Aston Pharmacy School
15 School of Life and Health Sciences
16 Aston University, Birmingham, UK. B4 7ET.
17 Tel: +44 (0) 121 204 3991
18 Fax: +44 (0) 121 359 0733
19 E-mail: y.perrie@aston.ac.uk

20

21

22 **Keywords:** Liposomes, microfluidics, poorly soluble drugs, bilayer loading, high
23 throughput

24

25

26

27

28

29

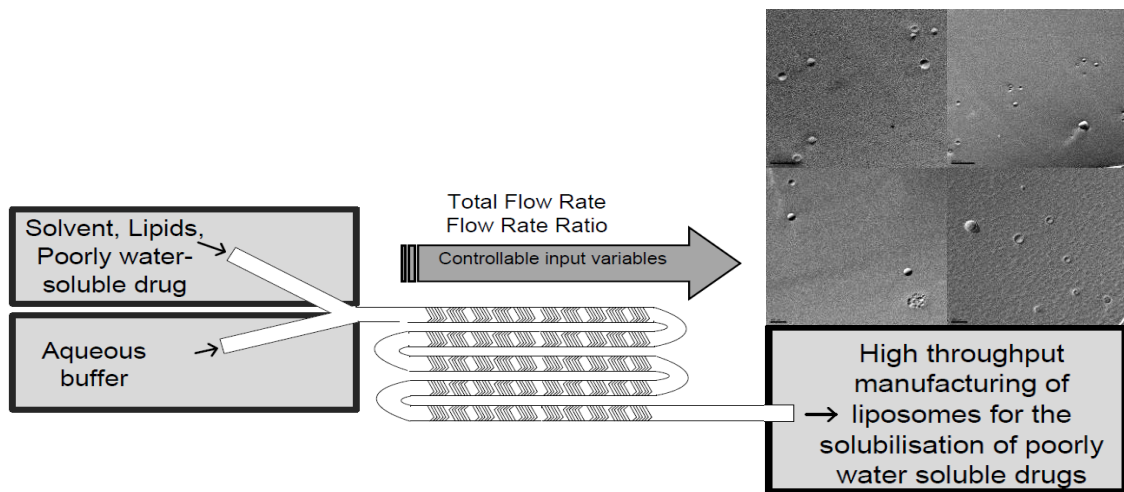
30

31

32

33

34 **Graphical Abstract**
35



36 **Abstract**

37 Besides their well-described use as delivery systems for water-soluble drugs,
38 liposomes have the ability to act as a solubilizing agent for drugs with low aqueous
39 solubility. However, a key limitation in exploiting liposome technology is the
40 availability of scalable, low-cost production methods for the preparation of
41 liposomes. Here we describe a new method, using microfluidics, to prepare
42 liposomal solubilising systems which can incorporate low solubility drugs (in this
43 case propofol). The setup, based on a chaotic advection micromixer, showed high
44 drug loading (41 mol%) of propofol as well as the ability to manufacture vesicles
45 with at prescribed sizes (between 50 to 450 nm) in a high-throughput setting. Our
46 results demonstrate the ability of merging liposome manufacturing and drug
47 encapsulation in a single process step, leading to an overall reduced process time.
48 These studies emphasise the flexibility and ease of applying lab-on-a-chip
49 microfluidics for the solubilisation of poorly water-soluble drugs.

50

51 **1 Introduction**

52 The delivery of drugs by liposomes was first described in the 1970s by Gregoriadis
53 (Gregoriadis and Ryman, 1971) and there is now a range of clinically approved
54 liposome-based products that improve the therapeutic outcome for patients.
55 Whilst liposomes are commonly considered for the delivery of aqueous soluble
56 drugs, they are also well placed to act as solubilisation agents for drugs with low
57 aqueous solubility. This is of considerable interest given that more than 40% of all
58 new chemical entities in discovery have low solubility and subsequent issues in
59 bioavailability (Savjani et al., 2012; Williams et al., 2012). The encapsulation of
60 low solubility drugs into the bilayer of liposomes allows not only for their
61 solubilisation in an aqueous media, but furthermore can offer protection from
62 degradation and control over the pharmacokinetic drug distribution profile and
63 improved therapeutic efficacy.

64

65 When solubilising drug within the liposomal bilayer, drug incorporation and
66 release rates has been shown to depend on the properties of the drug, the
67 composition of the liposomes, the lipid choice and concentration (Ali et al., 2010;
68 Ali et al., 2013; Mohammed et al., 2004). For example, the log P and molecular
69 weight are often considered to impact on bilayer loading, and studies have shown
70 that molecular weight may play a dominant role (Ali et al., 2013). When
71 considering the design of liposomes, there are a range of parameters that impact
72 on bilayer loading efficacy. For example, we have previously shown that
73 increasing the bilayer lipophilic volume (by adopting longer alkyl chain lipids
74 within the liposomes) increases the loading ability of liposomal systems
75 (Mohammed et al., 2004; Ali et al., 2013). Similarly, incorporation of charged
76 lipids within the liposomal system may also impact on bilayer loading through
77 electrostatic repulsion of drugs with like-charged liposomal bilayers (Mohammed
78 et al., 2004). Incorporation of cholesterol, whilst stabilising the liposomes was also
79 shown to inhibit bilayer drug loading (Ali et al., 2010) due to the space-filling
80 action of cholesterol in the liposomal bilayer. By increasing the orientation order
81 of the phospholipid hydrocarbon chains, cholesterol decreases bilayer
82 permeability. Indeed, the presence of cholesterol in liposomes solubilising
83 propofol was shown to shift the drug release profile from zero-order (when no

84 cholesterol was present) to first order (when 11 to 33 mol% of cholesterol was
85 incorporated). This maps to the idea that without cholesterol the bilayer can be
86 thought of as more 'porous' in nature compared with the more condensed and less
87 permeable cholesterol-containing liposome bilayers (Ali et al., 2010).

88

89 However, whilst a wide range of studies have looked at the effect of formulation
90 parameters on the application of liposomes as solubilising agents, more focus is
91 required into making liposomes a cost-effective solubilising agent. Recent
92 advances in lab-on-a-chip based tools for process development has already lead
93 to microfluidic-based methodologies in drug development (Dittrich and Manz,
94 2006; Weigl et al., 2003; Whitesides, 2006). Indeed, microfluidics-based methods
95 (which exploit controlled mixing of streams in micro-sized channels) have been
96 described for the manufacture of liposomes and lipid nanoparticles (van Swaay,
97 2013). Liposome formation by microfluidics primarily depends on the process of
98 controlled alterations in polarities throughout the mixer chamber, which is
99 followed by a nanoprecipitation reaction and the self-assembly of the lipid
100 molecules into liposomes. Generally, two or more inlet streams (lipids in solvent
101 and an aqueous phase) are rapidly mixed together and flow profiles in the
102 chamber itself are of low Reynolds numbers and categorized as laminar. Using
103 microfluidic systems a tight control of the mixing rates and ratio between aqueous
104 and solvent streams is achieved, with lower liquid volumes required, which
105 facilitates process development by reducing time and development costs. The
106 systems are designed with the option of high-throughput manufacturing and are
107 generally considered as less harsh compared to conventional methods of liposome
108 manufacturing that are based on mechanical disruption of large vesicles into small
109 and unilamellar ones (Wagner and Vorauer-Uhl, 2011). Within the range of
110 microfluidic mixing devices, we use a chaotic advection micromixer, a Staggered
111 Herringbone Micromixer (SHM). The fluid streams are passed through the series
112 of herringbone structures that allow for the introduction of a chaotic flow profile,
113 which enhances advection and diffusion. A chaotic advection micromixer, as well
114 as flow focusing methods, were shown to allow for scalability, associated with
115 defined vesicle sizes (Belliveau et al., 2012; Jahn et al., 2007). The method based
116 on chaotic advection was shown to reproducibly generate small unilamellar

117 liposomes (SUV) with tight control of the resulting liposome sizes at flow rates as
118 high as 70 mL/min in a parallelized mixer-setup. We have previously shown that
119 microfluidics can be used to produce cationic liposomal transfection agents
120 (Kastner et al., 2014), where design of experiments and multivariate analysis
121 revealed the ratio between aqueous and solvent phase having a strong relevance
122 for the formation of size-controlled liposomes. Within this study, we have
123 exploited microfluidics to develop a high-throughput manufacturing process to
124 prepare liposomes solubilising drug within their bilayer (Figure 1).

125

126 **2 Materials and Methods**

127 **2.1 Materials**

128 Egg Phosphatidylcholine (PC) and Cholesterol were obtained from Sigma-Aldrich
129 Company Ltd., Poole, UK. Ethanol and methanol were obtained from Fisher
130 Scientific UK, Loughborough, UK. TRIS Ultra Pure was obtained from ICN
131 Biomedicals, Inc., Aurora, Ohio. Propofol (2,6-Bis(isopropyl)phenol) and 5(6)-
132 Carboxyfluorescein (CF) was obtained from Sigma-Aldrich Company Ltd., Poole,
133 UK.

134

135 **2.2 Micromixer design and fabrication**

136 The micromixer was obtained from Precision NanoSystems Inc., Vancouver,
137 Canada. The mixer contained moulded channels which were 200 μm x 79 μm
138 (width x height) with herringbone features of 50 x 31 μm . 1 mL disposable
139 syringes were used for the inlet streams, with respective fluid connectors to the
140 chip inlets. Formulations using the micromixer were performed on a
141 NanoAssemblr™ (Precision NanoSystems Inc., Vancouver, Canada) that allowed
142 for control of the flow rates (0.5 to 6 mL/min) and the flow ratios (1:1 to 1:5, ratio
143 between solvent:aqueous) between the respective streams.

144 **2.3 Formulation of small unilamellar vesicles using microfluidics**

145 Lipids (16:4 molar ratio of PC and Cholesterol, 8:1 w/w) were dissolved in ethanol.
146 SUV were manufactured by injecting the lipids and aqueous buffer (TRIS 10mM,
147 pH 7.2) into separate chamber inlets of the micromixer. The flow rate ratio (FRR)
148 (ratio between solvent and aqueous stream) as well as the total flow rate (TFR) of

149 both streams were controlled by syringe pumps, calibrated to the syringe inner
150 diameter. FRR varied from 1:1 to 1:5 and TFR varied from 0.5 to 6 mL/min,
151 extrapolated from previous reported methods applying a SHM design with a
152 channel diameter of 200 μm (Kastner et al., 2014). The SUV formulation was
153 collected from the chamber outlet and dialysed at room temperature against TRIS
154 buffer (10mM, pH 7.2) for removal of residual solvent. The model drug of low
155 aqueous solubility was propofol (2,6-Bis(isopropyl)phenol), previously shown to
156 correspond to high encapsulation values in liposomal systems due to its low
157 molecular weight (Ali et al., 2013). To encapsulate propofol, the low solubility
158 drug was dissolved with the lipids in ethanol (0.5 to 3mg/mL) and thereby
159 liposome formation and encapsulation of the drug was performed simultaneously
160 using the micromixer method.

161

162 **2.4 Lipid film hydration and sonication**

163 Multilamellar vesicles (MLV) were prepared using the lipid film hydration method
164 (Bangham et al., 1965). Basically, lipids were dissolved in chloroform/methanol
165 (9:1 v/v) and the organic solvent was subsequently removed by rotary
166 evaporation under vacuum to form a dry lipid film which was flushed with N_2 to
167 ensure removal of solvent residues. The lipid film was hydrated with TRIS buffer
168 (10 mM, pH7.2) to form MLV. SUV were then formed via probe sonication
169 (Sonirep150plus, MSE; 5 min at an amplitude of 5).

170

171 **2.5 Measurement of particle characteristics**

172 Characterisation of the liposomes included size measurements using dynamic
173 light scattering (DLS) (Malvern NanoZS), reported as the z-average (intensity
174 based mean particle diameter) for monomodal size distributions and the zeta
175 potential using particle electrophoresis (Malvern NanoZS). Polydispersity (PDI)
176 measurements (Malvern NanoZS) were used to assess particle distribution.

177

178 **2.6 Quantification of drug concentrations**

179 Quantification of propofol was performed by reverse phase HPLC (Luna 5 μ C18,
180 Phenomenex, pore size of 100A, particle size of 5 μm). Detector was UV/Vis, at 268

181 nm. The flow rate was constant at 1.0 mL/min throughout with a gradient elution
182 from 5% B (Methanol), 95% A (0.1% Trifluoroacetic Acid (TFA) in water) to 100%
183 B over 10 minutes. HPLC-grade liquids were used, sonicated and filtered. The
184 column temperature was controlled at 35°C. All analysis was made in Clarity,
185 DataApex version 4.0.3.876. Quantification was achieved by reference to a
186 calibration curve produced from standards (six replicates in ethanol) at
187 concentrations from 0.01 to 1 mg/mL. The calibration curve had a linearity $R^2 \geq$
188 0.997, and all measurements were within the level of detection and level of
189 quantification.

190

191 **2.7 Determination of drug loading into liposomes**

192 The amount of drug loaded into the bilayer was measured by determination of the
193 residual amount of drug in the liposome bilayer after removal of non-entrapped
194 drug by dialysis (sink conditions) against 1 L of TRIS buffer, 10mM pH 7.2 (3500
195 Da, Medicell Membranes Ltd., London, UK). The drug content was measured by
196 HPLC as described in section 2.6. This protocol was validated by assessing the rate
197 of propofol removal by dialysis.

198

199 **2.8 Stability study**

200 For the stability study, formulations of propofol-loaded SUV were stored at 4°C,
201 25°C and 40°C in pharmaceutical grade stability cabinets over 60 days (time point
202 measurements at day 0, 7, 14, 21, 28 and 60). Samples were taken at these specific
203 time points for measurement of particle characteristics (section 2.5) and drug
204 loading (section 2.6). Samples were dialysed against 500 mL TRIS buffer (10 mM,
205 pH7.2, sink conditions) at each time point to remove non-entrapped propofol.
206 Propofol content remaining in the liposome formulation was assessed by HPLC as
207 described in section 2.6.

208

209 **2.9 Recovery of lipids and propofol**

210 To assess the overall lipid and propofol recovery in the microfluidics method, the
211 amount of lipid and propofol was measured by HPLC and expressed as % recovery
212 compared to the initial amount of lipids or propofol available in the stock. The

213 HPLC method was the same as described section 2.6, and lipids were quantified
214 by an evaporative light scattering (ELS) detector (Sedere, Sedex 90), set at 52°C
215 and coupled to the HPLC.

216

217 **2.10 Freeze Fracturing Imaging**

218 Two microlitres of liposome suspension were placed in a ridged gold specimen
219 support and frozen rapidly by plunging into a briskly stirred mixture of
220 propane:isopentane (4:1) cooled in a liquid nitrogen bath. Fracturing, with a cold
221 knife, and replication were performed in a Balzers BAF 400D apparatus under
222 conditions similar to those described previously for freeze-fracture of liposomes
223 (Forge et al., 1978; Forge et al., 1989). The replicas generated were floated off on
224 water, cleaned in domestic bleach diluted 1:1 in distilled water, and then washed
225 several times in distilled water before mounting on grids for electron microscopy.
226 The replicas were viewed in a JEOL 1200EXII transmission electron microscope
227 operating at 80kv and digital images collected with a Gatan camera. Images of the
228 freeze-fractured samples are presented in reverse contrast so that shadows
229 appear black. Fracturing imaging was performed by Prof. Andrew Forge at UCL
230 Ear Institute, London, UK.

231

232 **2.11 Drug release study**

233 The in-vitro release rate of the drug was determined by incubating the drug-
234 loaded liposomes in 1 L TRIS buffer (10mM, pH 7.2) after removal of the non-
235 incorporated drug, at 37°C in a shaking water bath (150 shakes/min). Three
236 independent formulations of drug-loaded liposomes made by the microfluidics
237 method (TFR 2 mL/min, FRR 1:3) and standard lipid film hydration followed by
238 sonication were incubated (3 mL per formulation) and samples of 200 µL were
239 withdrawn at time intervals of 0.5 h, 1 h, 2 h, 4 h, 8 h and 16 h. Drug quantification
240 was performed as described in section 2.6 and expressed as % cumulative release
241 relative to the initial amount of drug encapsulated.

242

243 **2.12 Incorporation of an aqueous marker within liposomes**

244 To validate the formulation of liposomes, the presence of an aqueous core within
245 the nanoparticles manufactured was verified by including and imaging of an
246 aqueous fluorescent dye. Liposomes were manufactured as described in section
247 2.3 and 2.4 with 1 mM Carboxyfluorescein (CF) included in the aqueous buffer
248 (TRIS, 10 mM, pH 7.2). Liposomes with entrapped CF were separated from un-
249 entrapped dye by dialysis over night against 1 L fresh TRIS buffer, pH 7.2.
250 Liposomes were imaged under a confocal microscope SP5 TCS II MP, Leica
251 Microsystems, Leica TCSSP5 II, 63x objective (HCX PLAPO 63x/1.4-0.6 oil CS).
252 Images were taken by Charlotte Bland, Aston University, ARCHA facility.

253

254 **2.13 Statistical tools**

255 If not stated otherwise, results were reported as mean \pm standard deviation (SD).
256 One- or two-way analysis of variance (ANOVA) was used to assess statistical
257 significance, followed by Tukeys multiple comparing test and t-test was
258 performed for paired comparisons. Significance was acknowledged for p values
259 less than 0.05 (marked with *). All calculations were made in GraphPad Prism
260 version 6.0 (GraphPad Software Inc., La Jolla, CA).

261

262 **3 Results and discussion**

263 **3.1 Influence of the flow rate ratio of aqueous and solvent stream on** 264 **liposome size**

265 The increase in polarity throughout the chamber drives the formation of small
266 unilamellar liposomes (SUV) in milliseconds of mixing. For their formation, the
267 rate of mixing as well as the ratio of aqueous to solvent stream has been
268 anticipated as crucial factors. The formation of the liposomes is based on a
269 nanoprecipitation reaction, where supersaturation occurs and the liposomes are
270 formed by self-assembly after aggregation of the lipid molecules. The initial aim of
271 this work was to assess the formation of liposomes by microfluidic mixing and
272 assess the efficacy of this system to act as a solubilising agent. Therefore,
273 liposomes were prepared from PC and Cholesterol (16:4 molar ratio, 8:1 w/w) at

274 different total flow rates (TFR) and flow rate ratios (FRR) and the size,
275 polydispersity and zeta potential were measured.

276

277 Liposomes formed at low flow rate ratio (1:1) showed the largest size of around
278 450 nm; increasing the flow rate ratio resulted in smaller liposomes (around 40 -
279 50 nm) at constant flow rates of 2 mL/min (TRIS, 10 mM, pH7.2) (Figure 2A).
280 However, increasing the flow rate ratio increased polydispersity (to a maximum
281 of 0.4; Figure 2B). Liposomes prepared at a flow rate ratio of 1:3 are shown in
282 Figure 2C, demonstrating their small nature, with average sizes of the vesicles in
283 agreement with average vesicle diameters obtained by particle sizing via dynamic
284 light scattering (~40 nm). In contrast, the smallest vesicle size of a comparable
285 formulation achievable via probe sonication with this lipid formulation was 100
286 nm in size at PDIs of 0.3 (data not shown). To verify the formation of liposomes,
287 rather than micelles, the liposomes made by the microfluidics method were
288 prepared encapsulating an aqueous fluorescent dye, carboxyfluorescein (CF, 1
289 mM), which was included in the aqueous phase during liposome manufacturing
290 by microfluidics and lipid film hydration. After removal of the free CF by dialysis
291 overnight, the remaining dye entrapped in the particles was visualized by confocal
292 microscopy. Bright green fluorescent cores visible in the particles manufactured
293 by the microfluidics method (Figure 2D) were in line with images obtained from
294 liposomes manufactured with the lipid film hydration method (images not
295 shown); which confirms the presence of aqueous cores and the formation of
296 liposomes in the novel microfluidics method.

297

298 These impact of flow rate ratio on vesicle size are in agreement with previous
299 work showing that the increase in FRR reduces the resulting size of the liposomes
300 (Jahn et al., 2010; Kastner et al., 2014; Zook and Vreeland, 2010). A correlation
301 between higher flow rate ratios and smaller liposome particles has been reported
302 using liposomes composed of 1-palmitoyl, 2-oleoyl phosphatidylcholine (POPC),
303 cholesterol and the triglyceride triolein, which resulted in the production of
304 vesicular structures with sizes ranging from 140 nm to 40 nm dependent on the
305 FRR chosen and triglyceride emulsions between 20– 50 nm size with nonpolar
306 cores (Zhigaltsev et al., 2012). The overall lower amount of residual solvent

307 present at higher FRR employed decreases the particle fusion (Ostwald ripening),
308 which leads to the formation of smaller particles (Zhigaltsev et al., 2012). The
309 increase in polydispersity may be a result of increased dilution at higher FRR
310 reducing the rate of diffusional mixing within the micromixer as noted in previous
311 studies applying a SHM mixer for liposome manufacturing (Kastner et al., 2014).
312 With diffusion being proportional to the lipid concentration, increasing FRR is
313 effectively reducing the lipid concentration, thus reducing the rate of diffusion,
314 leading to partly incomplete nucleation and a lower rate of liposome formation
315 inside the micromixer (Balbino et al., 2013b). Overall, these findings demonstrate
316 that a FRR of 1:2 to 1:4 result in liposomes of the smallest size and polydispersity.
317 The dilution factor (due to flow ratios chosen involved in the SHM method) is
318 overall lower compared to ratios employed in the flow-focusing method, which
319 can reach up to 60 (Jahn et al., 2010; Jahn et al., 2007; Jahn et al., 2004).
320 Furthermore, the SHM method enhances the diffusional mixing due to the
321 herringbone structures on the channel wall (Stroock et al., 2002), which results in
322 an enhanced mixing profiles compared to the flow-focusing technique.

323

324 **3.2 Influence of flow rate on throughput and particle characteristics**

325 To assess the ability of the system as a potential high-throughput manufacturing
326 method for liposomal solubilisation systems, we increased the total flow rate 3-
327 fold whilst maintaining the ratio between aqueous and solvent stream constant.
328 Liposome size was shown to be independent of the applied flow rate, with no
329 significant change in vesicle size (Figure 3A), pdi (Figure 3B) and zeta potential (-
330 $3\pm 2\text{mV}$; data not shown). These results support the suitability of microfluidics
331 manufacturing as a high throughput method with liposome characteristics being
332 maintained constant whilst increasing the total flow rate in the system. Our results
333 also confirm that the flow rate ratio used in the system is the most crucial variable
334 on liposome size, which has previously been demonstrated with other systems
335 (Balbino et al., 2013a; Balbino et al., 2013b; Jahn et al., 2007; Jahn et al., 2004;
336 Kastner et al., 2014). The scalability of the microfluidics method has been
337 suggested by Belliveau et al. 2013, by parallelization of the mixer chamber.
338 Scalability and increase in throughput together demonstrate the industrial

339 applicability comparable with scale-up options available (Wagner and Vorauer-
340 Uhl, 2011).

341

342 As shown, the increase in FRR is the main contributing factor governing liposome
343 size (Figure 2A). Nevertheless, an increase in FRR will inevitably lead to dilution
344 and lower liposome concentrations in the final liposome suspension produced. A
345 subsequent concentration process based on filtration (Pattnaik and Ray, 2009),
346 chromatography (Ruysschaert et al., 2005) or centrifugation adds additional
347 processing time. Therefore, to circumvent this additional process step, we
348 counteracted the dilution of the lipids at higher FRR by increasing initial lipid
349 concentrations introduced to the micromixer at the desired FRR. Through this
350 method, liposomes were manufactured at up to 6 fold higher concentrations.
351 Increased lipid concentrations at FRR of 1:3 and 1:5 did not significantly ($p>0.05$)
352 influence size and polydispersity compared to the standard lipid concentration
353 (Figure 4A and B), whereas at a FRR of 1:1 a significant ($p<0.05$) decrease in
354 vesicle size was observed (Figure 4A). At this lower FRR, the higher lipid
355 concentrations may again decreasing particle fusion leading to the formation of
356 smaller particles (Zhigaltsev et al., 2012). Nevertheless, this setup allows to
357 increase the final liposome concentration according to the FRR chosen without
358 adversely changing resulting vesicle size or polydispersity for the smallest vesicle
359 sizes obtained at higher FRR (Figure 4A and B respectively), due to the diffusional
360 mixing process in the SHM design.

361

362 **3.3 Drug loading studies: The effect of drug encapsulation by the liposome** 363 **manufacturing method**

364 So far, we have shown that the microfluidics method allows for size-controlled and
365 rapid synthesis of liposomes. To consider the applicability of this method to be
366 used for a high-throughput production of liposomes as solubilising agents the
367 loading capacity of the formulation was considered. Based on the optimisation
368 studies shown in Figure 2, propofol was solubilised within liposomes prepared at
369 a FRR of 1:3 and a TFR of 2 mL/min. The particle characteristics and drug loading
370 efficiency (mol%; Figure 5A) was determined at propofol concentrations ranging
371 from 0.5 to 3 mg/mL (effective concentration in the solvent stream).

372

373 Using a propofol concentration of 1 mg/mL in the solvent stream showed high
374 drug loading (~50 mol%), combined with particle size of ~50 nm and a low
375 polydispersity (Figure 5A). Particle size and polydispersity increased notably (ca.
376 600 nm and 0.8 respectively) at the highest propofol concentration (3 mg/mL in
377 the solvent stream, giving a loading of ~25mol%, Figure 5A), suggesting the
378 liposome system may have become saturated or destabilised at high propofol
379 concentrations (drug-to-lipid ratio 1.72 mol/mol). Based on this, subsequent
380 studies adopted a propofol concentration at 1 mg/mL in the solvent stream for all
381 performed encapsulation studies.

382

383 The drug encapsulation was further investigated as a function of FRR in the
384 microfluidics method. Propofol encapsulation (mol%) in liposomes prepared at
385 FRR 1:1, 1:3 and 1:5 remained at approximately 50 mol% with no statistical
386 difference. However this was significantly higher ($p < 0.0001$) than drug loading in
387 liposomes prepared via sonication (15 mol%; Figure 5B). The drug loading
388 efficiency of liposomes prepared by sonication is in line with previous reported
389 propofol encapsulation (Ali et al., 2013). Furthermore, drug encapsulation did not
390 alter vesicle size or polydispersity (Figure 5A) and vesicle sizes obtained by
391 dynamic light scattering were verified by freeze fracturing images (Figure 5D).
392 This higher drug loading may be a result of the highly efficient mixing processes
393 occurring during microfluidics that favours incorporation of propofol within the
394 bilayers in the same process as the vesicles form. Indeed, the here presented
395 method allows to achieve a propofol encapsulation of ~50 mol%, which
396 represents a total propofol amount of ~300 mg/mL in the final liposome
397 formulation, representing a 2000-fold increase to the reported aqueous solubility
398 of propofol, 150 $\mu\text{g/mL}$ (Altomare et al., 2003).

399

400 To consider, drug release profiles, the *in-vitro* release of propofol encapsulated in
401 liposomes by microfluidics was monitored at 37°C over 16 h. Liposomes formed
402 with the microfluidics method had a significant higher drug encapsulated at the
403 start of the release study (~55 mol%) compared to those vesicles formed by
404 sonication (20 mol% drug encapsulation). However, relative to initial loading, an

405 initial release of ca 40% was observed at 1 h for both formulations, followed by a
406 continuous release of 90% of the encapsulated drug was observed over 8 h (Figure
407 6). Whereas the fatty alcohol alkyl chain length was shown to affect the release
408 profile of encapsulated propofol (Ali et al., 2013), here the method of liposome
409 manufacturing was shown to mainly affect the amount of drug incorporated into
410 the liposomes, without altering the release profile of the encapsulated drug
411 against sink conditions. Previous we have shown that solubilisation of propofol in
412 phosphatidylcholine liposomes followed a zero-order release kinetics, where the
413 incorporation of a higher amount of cholesterol shifted the release rates towards
414 a first-order release model (Ali et al., 2010), implying that the release kinetics
415 itself are mainly dominated by the lipid composition and physicochemical
416 characteristics rather than the method of liposome manufacturing. This may
417 prove advantageous in the development of an IV formulation; the
418 pharmacokinetic release profile of propofol has been studied previously in a
419 colloidal dispersion between 20-100 nm (Cai et al., 2012), where rapid
420 distribution of propofol compared to the commercial product Diprivan®
421 highlighted the need on the development of new techniques for the encapsulation
422 of low solubility drugs.

423

424 It is important to verify both lipid and drug recovery when using the microfluidics
425 method, to ensure cost-effectiveness and that lipid and drug concentrations
426 remain locked at the ratio initially designed prior to formulation. To date, the
427 quantification of lipids is mainly dominated by time intensive assays like mass
428 spectrometry (Moore et al., 2007). Here, we introduce a simple and robust method
429 of lipid quantification based on evaporative light scattering (ELS) detection and
430 HPLC separation. We coupled an ELS detector downstream a HPLC separation
431 method, which allowed for quantification of any solids in the eluate with a lower
432 volatility than the mobile phase. Microfluidics based liposomal-drug formulations
433 showed good recovery of the drug (88 - 92%; Figure 5C), independent of the FRR.
434 Similarly, lipid recovery was high at FRR of 1:1 and 1:3 (97% and 89%; for FRR
435 1:1 and 1:3 respectively; Figure 5C). A significant drop (79%; $p < 0.01$) in lipid
436 recovery was noted at a flow ratio of 1:5, suggesting that higher FRR employed in
437 the microfluidics method may impede lipid recovery due to enhanced dilution in

438 the chamber. Nevertheless, the smallest vesicle size (~50nm) can be obtained at a
439 FRR of 1:3 (Figure 2A) and any further increase in FRR will not benefit the
440 formulation (size, pdi and drug encapsulation). Based on this, we chose the FRR
441 1:3 for a long-term stability study.

442

443 **3.4 The effect of manufacturing methods on liposome stability and drug** 444 **encapsulation over 8 weeks**

445 The SHM method was previously investigated for the encapsulation of a highly
446 soluble drug, with approximately 100% loading efficiencies being reported using
447 doxorubicin as a model drug (Zhigaltsev et al., 2012); the authors demonstrated
448 high drug retention of encapsulated drug with liposomes stored at 4°C over the
449 course of eight weeks (Zhigaltsev et al., 2012). Following the assessment that
450 liposomes manufactured by the microfluidics method yields significant higher
451 encapsulation of propofol, similarly we performed an eight-week stability study
452 to verify the integrity of the vesicles at different storage temperatures. Vesicles
453 were prepared using microfluidics as described above, and the initial amount of
454 propofol encapsulated was determined after removal of free drug by dialysis.
455 Vesicles were stored at 4°C, 25°C/60%RH and 40°C/75%RH (standard ICH
456 temperatures) in pharmaceutical grade stability cabinets and the formulations
457 made by the sonication method were stored at 25°C/60%RH (Figure 7, Table 1),
458 acting as the control method. The control liposomes formed by sonication showed
459 good stability in terms of size retention over the course of the study. Similarly, for
460 liposomes prepared using microfluidics, vesicle size remained unaffected after
461 storage over 8 weeks at 4°C and 25°C. In contrast, liposomes stored at 40°C
462 significantly increase in size from initially 55 nm to 120 nm (Figure 7A), with no
463 notable affect to polydispersity, suggesting the liposome population as a whole
464 has changed in size rather than a sub-set of the vesicles (Table 1).

465

466 Minor (but not significant) drug loss from the liposomes was detected for the
467 formulations at 4°C and 25°C after the first 7 days of storage (Figure 7B), after
468 which the formulations remained stable with final drug encapsulation values of
469 41±1 mol% and 41±4 mol% at 4°C and 25°C storage conditions respectively
470 (Figure 7B). Similarly, with liposomes formulated using sonication showed and

471 initial drug loss when stored at 25°C/60%RH which then plateaued out (Figure
472 7B). Notable drug loss from the microfluidic systems was only seen when they
473 were stored at elevated temperatures with the formulation stored at 40°C
474 showing almost complete drug loss over the course of the stability study, with only
475 5 ± 1 mol% drug remaining encapsulated after 8 weeks, similar to the final drug
476 encapsulated in the sonicated liposomes which were stored at 25°C/60%RH
477 (Figure 7B). Overall, vesicles produced with the microfluidics method were
478 smaller with a lower polydispersity than those obtained by lipid film hydration /
479 sonication. The vesicles manufactured by sonication maintained their size around
480 100 ± 20 nm throughout the stability study (stored at 25°C) as well as their
481 polydispersity (Table 1). Results suggest that the method of manufacturing mainly
482 impacts the drug encapsulation rather than the physical properties (size, pdi, zeta
483 potential). Stability of the formulations is crucial and these results demonstrate
484 that liposomes formed by the microfluidics method remain over two months at
485 conditions of 4 and 25°C.

486

487 **3.5 Conclusion**

488 Here, for the first time, we have demonstrated a high-throughput, robust method
489 of preparing size-controlled liposomes as solubilising agents using microfluidics.
490 These liposomes have well defined, scalable, process controlled, physico-chemical
491 attributes demonstrating this method is suitable for pre-clinical and clinical
492 production of liposomes. Drug loading was shown to be in an applicable range for
493 clinical application (Biebuyck et al., 1994). Furthermore, using this novel method,
494 liposome manufacturing and drug encapsulation are processed in a single process
495 step, circumventing an additional drug loading step downstream, which notably
496 reduces the time for production of stable drug-loaded vesicles of specified
497 physico-chemical characteristics.

498

499 **3.6 Acknowledgements**

500 Prof. Andrew Forge (UCL Ear Institute, London, UK) is acknowledged for the
501 imaging of the liposomes by freeze fracturing. Charlotte Bland (Aston University,
502 ARCHA facility) is acknowledged for the imaging of liposomes by fluorescent

503 microscopy. This work was part funded by the EPSRC Centre for Innovative
504 Manufacturing in Emergent Macromolecular Therapies and Aston University.
505

506 **References**

- 507 Ali, M.H., Kirby, D.J., Mohammed, A.R., Perrie, Y., 2010. Solubilisation of drugs
508 within liposomal bilayers: alternatives to cholesterol as a membrane stabilising
509 agent. *Journal of pharmacy and pharmacology* 62, 1646-1655.
- 510 Ali, M.H., Moghaddam, B., Kirby, D.J., Mohammed, A.R., Perrie, Y., 2013. The
511 role of lipid geometry in designing liposomes for the solubilisation of poorly
512 water soluble drugs. *International journal of pharmaceutics* 453, 225-232.
- 513 Altomare, C., Trapani, G., Latrofa, A., Serra, M., Sanna, E., Biggio, G., Liso, G.,
514 2003. Highly water-soluble derivatives of the anesthetic agent propofol: in vitro
515 and in vivo evaluation of cyclic amino acid esters. *European journal of*
516 *pharmaceutical sciences* 20, 17-26.
- 517 Balbino, T.A., Aoki, N.T., Gasperini, A.A., Oliveira, C.L., Azzoni, A.R., Cavalcanti,
518 L.P., de la Torre, L.G., 2013a. Continuous flow production of cationic liposomes
519 at high lipid concentration in microfluidic devices for gene delivery applications.
520 *Chemical Engineering Journal* 226, 423-433.
- 521 Balbino, T.A., Azzoni, A.R., de La Torre, L.G., 2013b. Microfluidic devices for
522 continuous production of pDNA/cationic liposome complexes for gene delivery
523 and vaccine therapy. *Colloids and Surfaces B: Biointerfaces* 111, 203-210.
- 524 Bangham, A., Standish, M.M., Watkins, J., 1965. Diffusion of univalent ions
525 across the lamellae of swollen phospholipids. *Journal of molecular biology* 13,
526 238-IN227.
- 527 Belliveau, N.M., Huft, J., Lin, P.J., Chen, S., Leung, A.K., Leaver, T.J., Wild,
528 A.W., Lee, J.B., Taylor, R.J., Tam, Y.K., 2012. Microfluidic synthesis of highly
529 potent limit-size lipid nanoparticles for in vivo delivery of siRNA. *Molecular*
530 *Therapy—Nucleic Acids* 1, e37.
- 531 Biebuyck, J.F., Smith, I., White, P.F., Nathanson, M., Gouldson, R., 1994.
532 Propofol: an update on its clinical use. *Anesthesiology* 81, 1005-1043.
- 533 Cai, W., Deng, W., Yang, H., Chen, X., Jin, F., 2012. A propofol microemulsion
534 with low free propofol in the aqueous phase: Formulation, physicochemical
535 characterization, stability and pharmacokinetics. *International journal of*
536 *pharmaceutics* 436, 536-544.
- 537 Dittrich, P.S., Manz, A., 2006. Lab-on-a-chip: microfluidics in drug discovery.
538 *Nature Reviews Drug Discovery* 5, 210-218.
- 539 Forge, A., Knowles, P., Marsh, D., 1978. Morphology of egg
540 phosphatidylcholine-cholesterol single-bilayer vesicles, studied by freeze-etch
541 electron microscopy. *The Journal of membrane biology* 41, 249-263.
- 542 Forge, A., Zajic, G., Davies, S., Weiner, N., Schacht, J., 1989. Gentamicin alters
543 membrane structure as shown by freeze-fracture of liposomes. *Hearing*
544 *research* 37, 129-139.
- 545 Gregoriadis, G., Ryman, B., 1971. Liposomes as carriers of enzymes or drugs:
546 a new approach to the treatment of storage diseases. *Biochem. J* 124.
- 547 Jahn, A., Stavis, S.M., Hong, J.S., Vreeland, W.N., DeVoe, D.L., Gaitan, M.,
548 2010. Microfluidic mixing and the formation of nanoscale lipid vesicles. *Acs*
549 *Nano* 4, 2077-2087.
- 550 Jahn, A., Vreeland, W.N., DeVoe, D.L., Locascio, L.E., Gaitan, M., 2007.
551 Microfluidic directed formation of liposomes of controlled size. *Langmuir* 23,
552 6289-6293.

553 Jahn, A., Vreeland, W.N., Gaitan, M., Locascio, L.E., 2004. Controlled vesicle
554 self-assembly in microfluidic channels with hydrodynamic focusing. *Journal of*
555 *the American Chemical Society* 126, 2674-2675.

556 Kastner, E., Kaur, R., Lowry, D., Moghaddam, B., Wilkinson, A., Perrie, Y., 2014.
557 High-throughput manufacturing of size-tuned liposomes by a new microfluidics
558 method using enhanced statistical tools for characterization. *International*
559 *Journal of Pharmaceutics*.

560 Mohammed, A., Weston, N., Coombes, A., Fitzgerald, M., Perrie, Y., 2004.
561 Liposome formulation of poorly water soluble drugs: optimisation of drug
562 loading and ESEM analysis of stability. *International Journal of Pharmaceutics*
563 285, 23-34.

564 Moore, J.D., Caufield, W.V., Shaw, W.A., 2007. Quantitation and
565 standardization of lipid internal standards for mass spectroscopy. *Methods in*
566 *enzymology* 432, 351-367.

567 Pattnaik, P., Ray, T., 2009. Improving liposome integrity and easing bottlenecks
568 to production. *Pharmaceutical Technology Europe* 22.

569 Ruyschaert, T., Marque, A., Duteyrat, J.-L., Lesieur, S., Winterhalter, M.,
570 Fournier, D., 2005. Liposome retention in size exclusion chromatography. *BMC*
571 *biotechnology* 5, 11.

572 Savjani, K.T., Gajjar, A.K., Savjani, J.K., 2012. Drug solubility: importance and
573 enhancement techniques. *ISRN pharmaceutics* 2012.

574 Stroock, A.D., Dertinger, S.K., Ajdari, A., Mezić, I., Stone, H.A., Whitesides,
575 G.M., 2002. Chaotic mixer for microchannels. *Science* 295, 647-651.

576 van Swaay, D., 2013. Microfluidic methods for forming liposomes. *Lab on a*
577 *Chip* 13, 752-767.

578 Wagner, A., Vorauer-Uhl, K., 2011. Liposome technology for industrial
579 purposes. *J Drug Deliv* 2011, 591325.

580 Weigl, B.H., Bardell, R.L., Cabrera, C.R., 2003. Lab-on-a-chip for drug
581 development. *Advanced drug delivery reviews* 55, 349-377.

582 Whitesides, G.M., 2006. The origins and the future of microfluidics. *Nature* 442,
583 368-373.

584 Williams, R.O., Watts, A.B., Miller, D.A., 2012. Formulating poorly water soluble
585 drugs. Springer.

586 Zhigaltsev, I.V., Belliveau, N., Hafez, I., Leung, A.K., Huft, J., Hansen, C., Cullis,
587 P.R., 2012. Bottom-up design and synthesis of limit size lipid nanoparticle
588 systems with aqueous and triglyceride cores using millisecond microfluidic
589 mixing. *Langmuir* 28, 3633-3640.

590 Zook, J.M., Vreeland, W.N., 2010. Effects of temperature, acyl chain length,
591 and flow-rate ratio on liposome formation and size in a microfluidic
592 hydrodynamic focusing device. *Soft Matter* 6, 1352-1360.

593
594

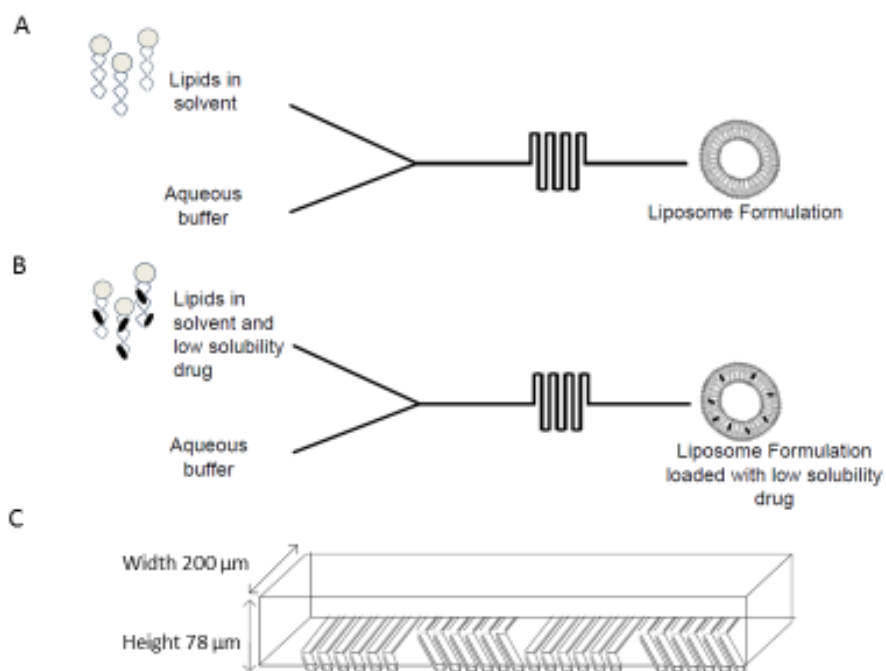
595 **Tables**

596 Table 1: Polydispersity at different storage conditions for 8 weeks. Results are
 597 mean out of triplicate formulations and measurements.

Day	0	7	14	21	28	60
<u>Microfluidics</u>						
4°C	0.403 ± 0.02	0.286 ± 0.01	0.282 ± 0.01	0.295 ± 0.01	0.261 ± 0.01	0.305 ± 0.01
25°C	0.403 ± 0.02	0.295 ± 0.01	0.279 ± 0.01	0.301 ± 0.04	0.302 ± 0.03	0.266 ± 0.03
40°C	0.403 ± 0.02	0.254 ± 0.001	0.121 ± 0.02	0.119 ± 0.001	0.129 ± 0.01	0.221 ± 0.01
<u>Sonication</u>						
25°C	0.656 ± 0.02	0.652 ± 0.02	0.522 ± 0.15	0.658 ± 0.049	0.552 ± 0.04	0.505 ± 0.06

598

599 **Figures**
600



601 **Figure 1**

602 Figure 1: Schematic depiction of the liposome formation process based on the
603 SHM design, a chaotic advection micromixer for (A) empty liposomes, (B) drug
604 loaded liposomes and (C) chamber layout.
605

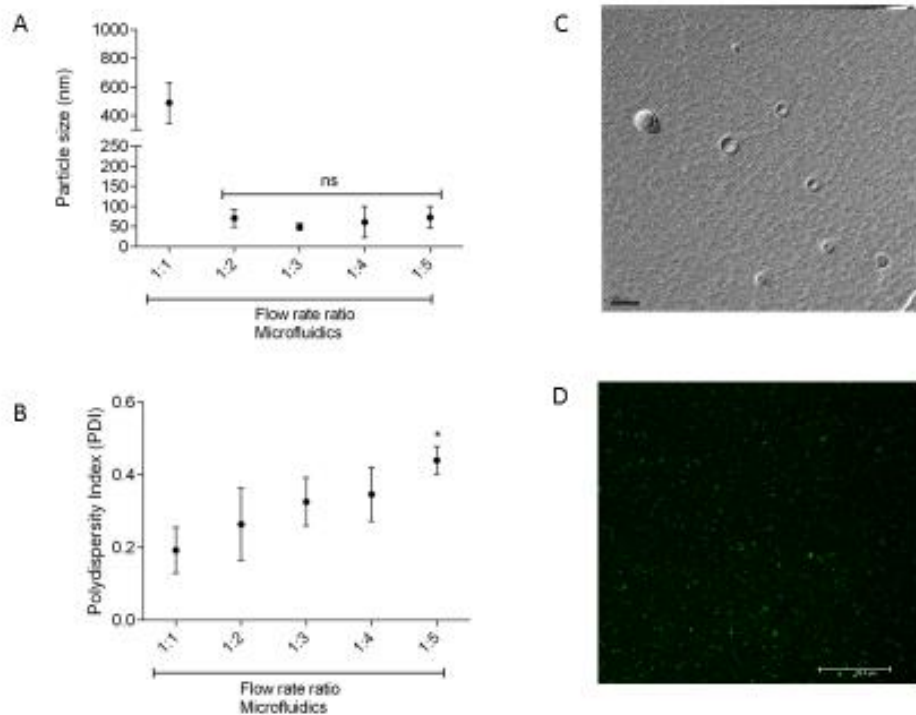


Figure 2

606

607 Figure 2: Liposome size (A) and polydispersity (B) of vesicles formulated with

608 microfluidics method at increasing flow ratios. ns = not significant ($p > 0.05$), *

609 denotes statistical significance ($p < 0.05$) in comparison to FRR 1:1 (C) Freeze

610 fracturing electron microscopy images for empty liposomes manufactured with

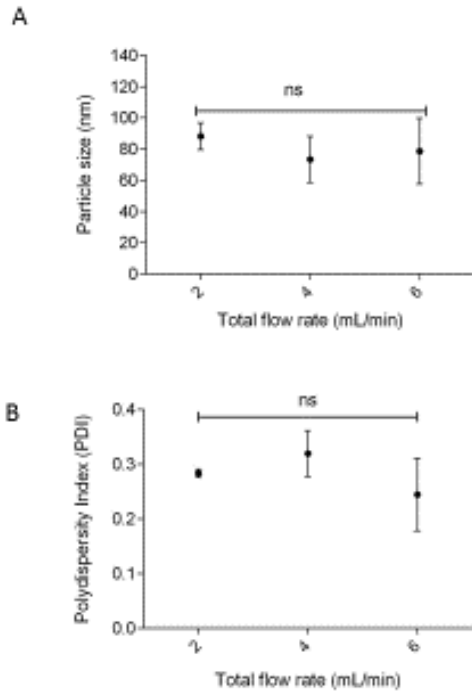
611 the microfluidics method. Bar represents 100 nm. (D) Fluorescent microscope

612 images of liposomes manufactured with the microfluidics method,

613 carboxyfluorescein was encapsulated within the aqueous core of the vesicles as a

614 control for the manufacturing of bilayer liposomes. Bar represents 20 μm.

615



616 **Figure 3**
 617 Figure 3: Liposome size (A) and polydispersity (B) of vesicles formulated with
 618 microfluidics at increasing flow rates and constant flow ratio of 1:3, n = 3, ns = not
 619 significant (p>0.05).
 620
 621

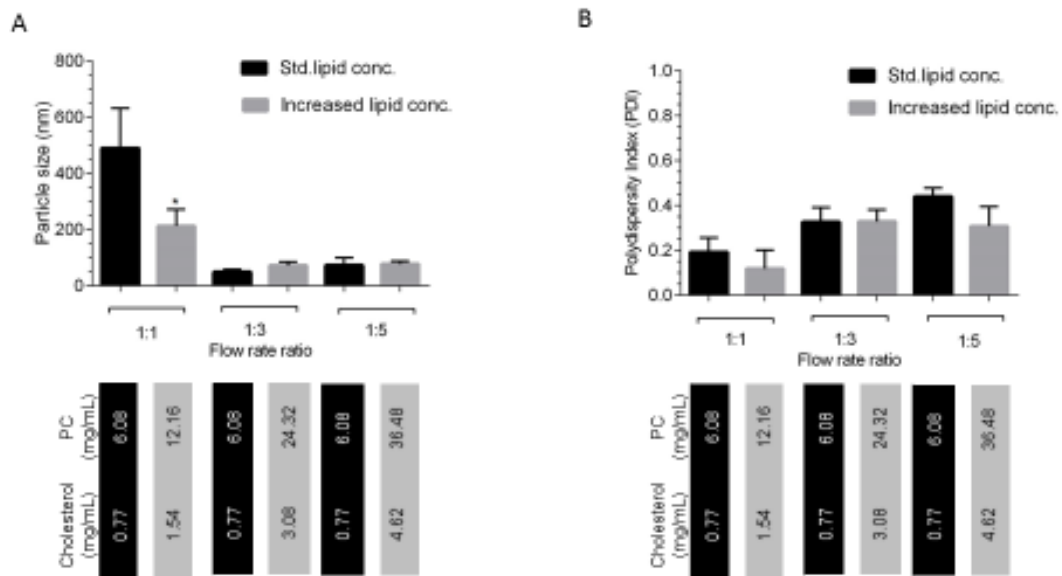
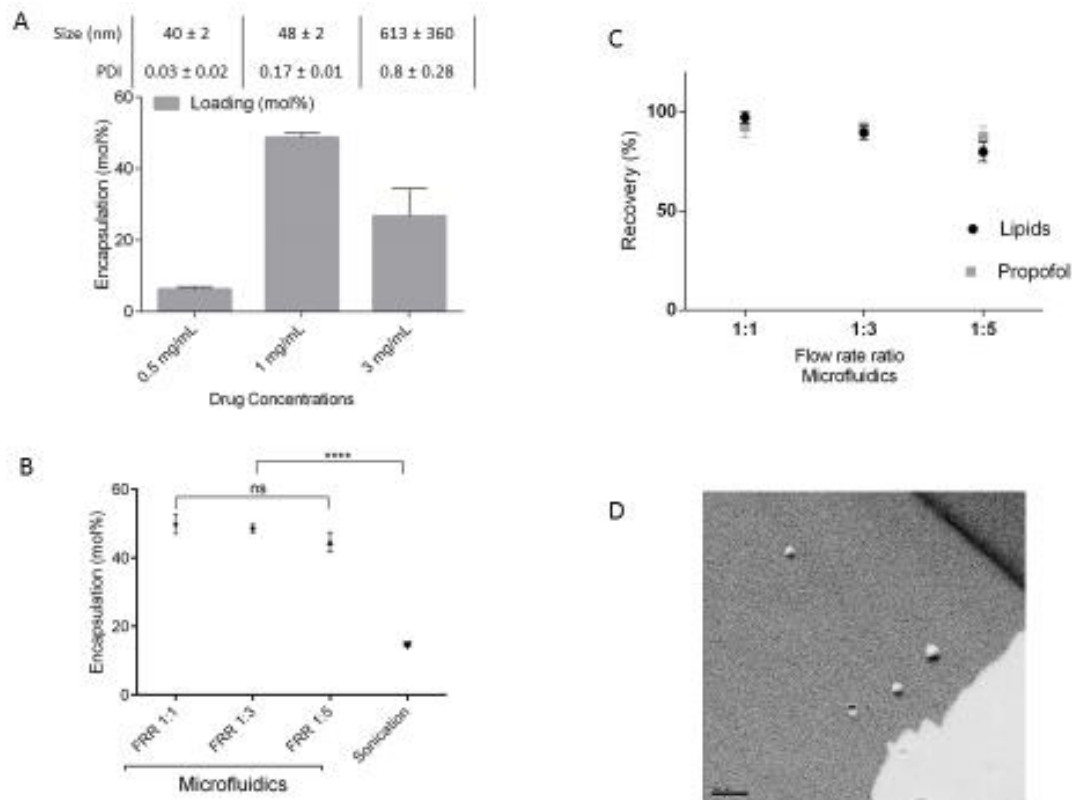


Figure 4

622

623 Figure 4: Increase in the lipid concentration in the ethanol stock to circumvent
 624 the dilution effect at flow ratios of 1:1, 1:3 and 1:5 for (A) liposome size, * denotes
 625 statistical significance ($p < 0.05$) in comparison to FRR 1:1 for the standard lipid
 626 concentration and (B) polydispersity with respective concentration of PC and
 627 Cholesterol in the inlet stream, $n = 3$.

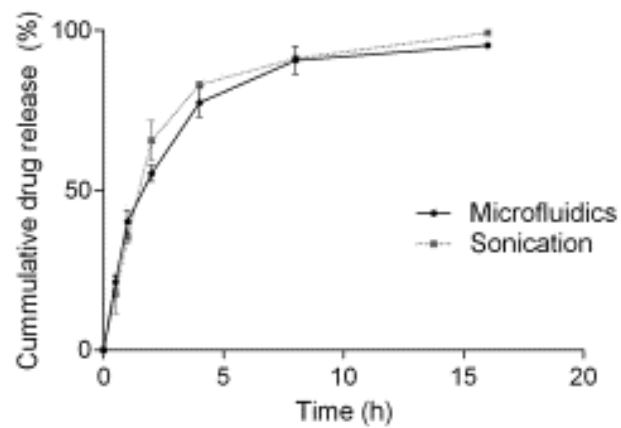
628



629

Figure 5

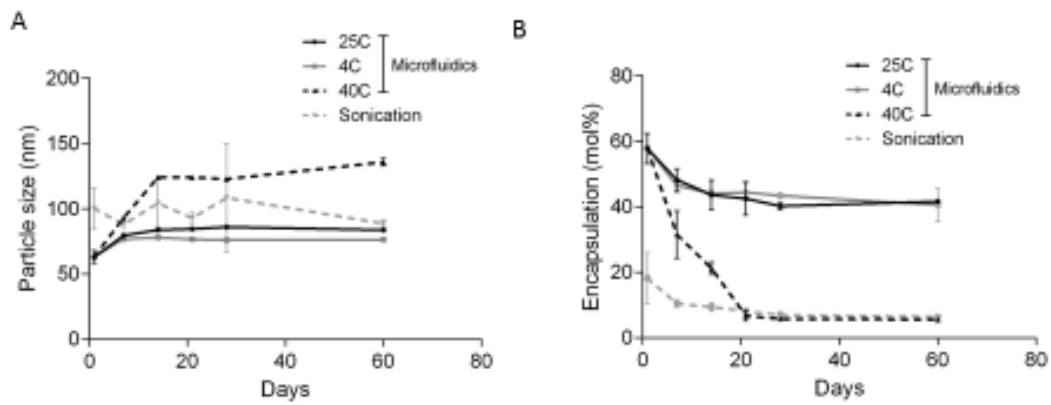
630 Figure 5: (A) Effect of drug concentrations in the ethanol inlet stream (0.5, 1 and
631 3 mg/mL) on encapsulation efficiency (mol%), particle size and polydispersities
632 at a flow ratio of 1:3. (B) Encapsulation efficiency (mol%) of liposomes formed
633 with the microfluidics method at flow ratios of 1:1, 1:3 and 1:5 compared to the
634 encapsulation efficiency using the sonication method. Results are average out of
635 triplicate formulations and measurements. ns = not significant ($p > 0.05$), * denotes
636 statistical significance ($p < 0.00001$) in comparison to microfluidics-based
637 samples. (C) Recovery of lipids and propofol in the microfluidics method at
638 different flow ratios. Results are expressed as % compared to the initial lipid and
639 propofol amount present ($n = 3$). (D) Freeze fracturing electron microscopy
640 images for liposomes loaded with the low solubility model drug (propofol)
641 manufactured with the microfluidics method. Bar represents 100 nm
642



643 **Figure 6**

644 Figure 6: Effect of manufacturing method to the drug release of propofol from
645 liposomes. Results show the cumulative drug release profile from formulations
646 manufactured with the standard lipid film hydration / sonication method and
647 microfluidics and represent percentage cumulative release of initially entrapped
648 propofol, expressed as the means of three experiments \pm SD.

649



650 **Figure 7**
 651 Figure 7: Size (A) and drug encapsulation (mol%) (B) at different storage
 652 conditions over 8 weeks. Results are mean of triplicate formulations and
 653 measurements.